Hindawi
Journal of Nanomaterials
Volume 2022, Article ID 3530620, 13 pages
https://doi.org/10.1155/2022/3530620

Research Article

Establishment of FK506-Enriched PLGA Nanomaterial Neural Conduit Produced by Electrospinning for the Repair of Long-Distance Peripheral Nerve Injury

Ting-Min Xu,[1,2,3] Hong-Yu Chu,[4] Ming Li,[5,6,7] Zuliyaer Talifu,[1,2,3] Han Ke,[1,2,3] Yun-Zhu Pan,[1,2,3] Xin Xu,[1,2,3] Yan-hua Wang,[6,7,8] Wei Guo,[5,6,7] Chuan-Lin Wang,[5,6,7] Feng Gao,[1,2,3] and Jian-Jun Li[1,2,3]

[1]*School of Rehabilitation Medicine, Capital Medical University, Beijing 100068, China*
[2]*Department of Spinal and Neural Function Reconstruction, Beijing Bo'ai Hospital, Rehabilitation Research Center, Beijing 100068, China*
[3]*Beijing Key Laboratory of Neural Injury and Rehabilitation, Beijing 100068, China*
[4]*Department of Comprehensive Rehabilitation, China Rehabilitation Research Center, Beijing 100068, China*
[5]*Trauma Medicine Center, Peking University People 's Hospital, Beijing 100044, China*
[6]*Key Laboratory of Trauma and Neural Regeneration(Peking University, Ministry of Education, Beijing 100044, China*
[7]*National Center for Trauma Medicine, Beijing 100044, China*
[8]*Department of Trauma and Orthopedics, Peking University People 's Hospital, Beijing 100044, China*

Correspondence should be addressed to Feng Gao; gaofeng5960@126.com and Jian-Jun Li; crrclijj@163.com

Ting-Min Xu, Hong-Yu Chu, and Ming Li contributed equally to this work.

Received 24 June 2022; Accepted 28 July 2022; Published 22 August 2022

Academic Editor: Xiaoming Li

Peripheral nerve injury (PNI) is a serious complication of trauma. Autologous nerve transplantation is the gold standard for the treatment of long-distance peripheral nerve defects, but is often limited by insufficient donor sites, postoperative pain, and paresthesia at the donor site. Peripheral nerve tissue engineering has led to the development of neural conduits to replace autologous nerve grafts. This study aimed to evaluate a new type of electrospun nanomaterial neural conduit, enriched with tacrolimus (FK506), which is an FDA-approved immunosuppressant, for the repair of long-distance peripheral nerve injuries. Poly (lactic-co-glycolic acid) (PLGA) nanofibrous films, with FK506, were prepared by electrostatic spinning and rolled into hollow cylindrical nerve vessels with an inner diameter of 1 mm and length of 15 mm. Material characterization, mechanical testing, degradation, drug release, cytotoxicity, cell proliferation, and migration assays were performed in vitro. Long-distance sciatic nerve injuries in rats were repaired in vivo using electrospun nerve conduit bridging, and nerve regeneration and muscle and motor function recovery were evaluated by gait analysis, electrophysiology, and neuromuscular histology. Compared to PLGA, the PLGA/FK506 nanomaterial neural conduit showed little change in morphology, mechanical properties, and chemical structure. In vitro, PLGA/FK506 showed lower cytotoxicity and better biocompatibility and effectively promoted the proliferation, adhesion, and migration of Schwann cells. In vivo, PLGA/FK506 had a better effect on sciatic nerve index, compound muscle action potential intensity and delay time, and nerve regeneration quality 12 weeks post-transplantation, effectively promoting long-distance defect sciatic nerve regeneration and functional recovery in rats. FK506-enriched PLGA nanomaterial neural conduits offer an effective method for repairing long-distance peripheral nerve injury and have potential clinical applications.

1. Introduction

Peripheral nerve injury (PNI) is clinically common and results in loss of motor and/or sensory function, which has a serious effect on the prognosis and quality of life of patients [1–3]. Autologous nerve transplantation has many problems, including limited sources, functional destruction of nerve donor sites, and many clinical complications, whereas allogeneic nerve transplantation has inevitable immune rejection problems [4]. In recent years, tissue engineering nerve conduits with properties beyond autologous nerve grafts have become a potential alternative for repair after PNI [5, 6].

The preparation of neural conduits with excellent performance requires comprehensive consideration of the morphological design, material selection, manufacturing technology, and parameter fine-tuning of the experimental scheme of the conduits to simulate the pipeline microenvironment of nerve regeneration to the greatest extent and promote rapid regeneration and functional control of peripheral nerves [7–9]. Nano-micro scaffolds, made by electrostatic spinning technology, have high specific surface area and porosity, which can better simulate the mechanism of the extracellular matrix and provide a good microenvironment for the effective release of neurotrophins and the rapid growth of nerve cells [10, 11]. The effectiveness of rolling obtained nerve membranes into hollow, multilayer, tubular, and artificial nerve conduits for PNI has been proven in various studies [12, 13].

Poly (lactic-co-glycolic acid) (PLGA), as a common wound suture material certified by the FDA [14–16] and a common tissue engineering material, has been widely used in clinical practice, with great advantages in its mechanical properties and degradation performance. Its proper flexibility, stiffness, and good biocompatibility are conducive to the migration of Schwann cells and endothelial cells [17, 18]. PLGA nanofibers, prepared using electrostatic spinning technology, are an ideal material for the construction of neural conduit scaffolds.

The repair of PNI is inseparable from excellent microsurgical techniques. Currently, epineurium sutures are the main PNI repair technology used clinically, but they have many problems, such as generation of neuromas, nerve misconnection, and mismatch. The resultant effect of nerve repair is far less than expected [1]. Through a series of studies, Jiang Baoguo et al. found that artificial nerve conduits can help guide the axons of peripheral nerves to achieve axial growth. Meanwhile, accurate nerve docking was achieved using the selective regeneration characteristics of peripheral nerves, which effectively reduced the growth of neuromas and the occurrence of long-term peripheral neuralgia and became a successful alternative to traditional peripheral nerve epineurium suturing [19, 20]. Previous research found that in PNI, the broken blood-nerve barrier and axonal exposure to the body fluid environment caused increased local exudation and inflammatory reactions, aggravating secondary injury, degeneration, and necrosis of the nerve, causing neuropathic pain, further affecting the quality of nerve regeneration and repair [21]. Therefore, the inhibition of an overactive immune response at the nerve injury site is essential for the repair of that injury. Tacrolimus (FK506), an FDA-approved immunosuppressant, has been shown to enhance peripheral nerve regeneration. Furthermore, Davis et al. found in his study that multifunctional FK506 embedded, micropatterned PLGA films have potential to be used in the construction of peripheral nerve repair devices [22]. Also, FK506-enriched nanoneural conduits developed by electrospinning technology have been proven to effectively reduce neuroimmune response and promote nerve regeneration [23].

This study aimed to evaluate a new type of nanomaterial neural conduit, enriched with FK506, for the repair of long-distance peripheral nerve injuries.

2. Materials and Methods

2.1. Preparation and Characterization of Electrospinning PLGA Nanofiber Membranes and FK506-Enriched Neural Conduits. 1 g of PLGA (purchased from Jinan Dagang Co., Ltd., Jinan, China) particles was dissolved in 10 mL of mixed solvent (7 : 3, v/v) with trichloromethane (purchased from McLean Reagent Co., Ltd., Beijing, China) and N, N-dimethylformamide (purchased from McLean Reagent Co., Ltd., Beijing, China) and stirred at room temperature for 5 h until the PLGA dissolved completely; it was then prepared as a 10% electrospinning solution.

FK506 (purchased from Selleck, Shanghai, China) was predissolved in dimethyl sulfoxide (DMSO), and a solution with a concentration of 40 μg/mL was prepared. Then, 1 mL of the FK506 solution was added to the electrospinning solution and stirred for 5 h (500 RPM). This solution was loaded into a 20-mL syringe, and the spinning voltage of the electrospinning machine was set at 20 kV, the flow rate of the solution was set at 0.5 mL/h, the distance of the receiving device was set at 16 cm, the temperature was set at 25°C, and the humidity was set at 40%. FK506-enriched PLGA nanofiber membranes, with a thickness of 0.1 mm, were obtained. The membranes were cut into small pieces, prepared, and rolled by a steel needle into a hollow cylindrical nerve conduit with an inner diameter of 1 mm and a length of 15 mm.

2.1.1. Morphology Testing of the Nanofiber Membrane. The nanofibers were cut into appropriate sizes and gold-sprayed for 60 seconds. The morphologic characteristics of the nanofibers were examined using scanning electron microscopy (SEM). In addition, the diameter distribution of the nanofibers in the SEM images was analyzed using ImageJ software.

2.1.2. Fourier Transform Infrared Spectrometry. PLGA and PLGA/FK506 nanofibers were tested in the range of 4000-600 cm^{-1} using ATR-FTIR to analyze the chemical structure of the nanofibers.

2.1.3. Mechanical Properties Measurement. The nanofibers were cut into 50 mm × 20 mm pieces. The thickness of each sample was measured using a spiral micrometer, and the mechanical properties of the nanofibers were tested with a tensile tester. The tensile speed used was 10 mm/min.

The other organic reagents used in this part of the study were purchased from Sinopharm (Beijing, China). Other biological reagents were purchased from Sangong Bioengineering Co., Ltd. (Shanghai, China). The equipment used included a field emission SEM (Hitachi SU8010, Japan), an energy scattering spectrometer (EDS, IXRF SDD3030), Fourier transform infrared spectrometer (FTIR, Thermo Scientific, Nicolet 6700, USA), a tension tester (MarK-10, ESM303 motorized tension/compression test stand, USA), and a confocal laser microscope (Olympus FV1000, Japan).

2.2. Performance Evaluation of In Vitro Degradation and Drug Release of the Nerve Conduits. A certain mass of PLGA and PLGA/FK506 nanofiber membranes was weighed, and the initial mass of the sample was recorded as M_0. The samples were placed into a 10-mL phosphate buffered saline (PBS) solution and oscillated in a shaker at 37°C and 100 RPM. The scaffolds were removed in the first, second, third, fourth, and fifth weeks. The samples were washed with deionized water, freeze-dried, and weighed, and the mass after degradation was recorded as M_1. The degradation efficiency was calculated according to the following formula:

$$\text{Degradation Efficiency}(\%) = \frac{M0 - M1}{M0} \times 100\%. \quad (1)$$

Each group of samples was tested three times and the results were averaged.

The release behavior of FK506 from PLGA/FK506 nanofibers was measured. First, the FK506 DMSO solution was diluted with PBS into standard solutions of 140, 120, 100, 80, 60, 40, and 20 μg/mL. The FK506 solution of each concentration was placed in a 96-well plate, and the standard curve was measured three times for each concentration. The 60 mg nanofiber membrane was immersed in a 3-mL PBS solution (7.2-7.4), and all the released solution was taken out at certain time points. The released amount was determined using a UV spectrophotometer (HV-VIS, Hitachi U-4100), and 3 mL fresh PBS solution was added for the next test.

2.3. Evaluation of the Safety and Effectiveness of the Nerve Conduits in In Vitro Cell Experiments. Good biocompatibility is an important index for the evaluating neural conduits. In this study, the MTT (3-(4,5-dimethylthiazol-2-yl)-2,5-diphenyltetrazolium bromide) assay and cell viability staining were used to evaluate the biocompatibility of the materials. Mouse embryonic fibroblast (NIH/3T3) cells were purchased from the National Infrastructure of Cell Line Resource (Beijing, China) and cultured in Dulbecco's modified eagle medium (DMEM) high glucose (Gibco, Carlsbad, CA, USA) with added 10% fetal bovine serum (Gibco) and 1% penicillin-streptomycin (Gibco). The cell suspension was diluted to 1×10^4/mL. Cell suspensions (100 μL) were added to each well of the 96-well plates, and the nanofiber nerve conduit samples were then added to obtain concentrations of 5000, 2500, 1250, 625, 312.5, and 156.25 μg/mL. Five parallel experiments were conducted for each group of cells, and the materials and cells were co-cultured for 24 h. Thereafter, 10 mL MTT reagent was added to each well, and the culture was continued for 4 h. Then, the cell culture plate was removed, the supernatant was removed, and 100 μL DMSO solution was added to each well. The optical density (OD) values of the cells were measured using an enzyme standard instrument (SpectraMaxM2, Molecular Devices, Sunnyvale, CA, USA).

To further evaluate the effectiveness and safety of the neural conduits, the proliferation, adhesion, and migration of Schwann cells on the conduits were observed. Rat Schwann cells (ATCC CRL-2765, rat Schwann cell lines) were purchased from the cell bank of the Chinese Academy of Sciences (Shanghai, China) and cultured in DMEM high glucose (Gibco, Carlsbad, CA, USA) supplemented with 10% fetal bovine serum (Gibco) and 1% penicillin-streptomycin (Gibco). The nanofiber material was sterilized for 1 h, and the PBS buffer was fully watered and washed three times. The residual ethanol was removed, and the scaffold was immersed in a completely prepared medium for later use. Schwann cells in culture vials were then digested with trypsin, diluted to a concentration of 10^4 cells per well, and inoculated into the nanofiber membranes.

On the second day after cell seeding, the morphology of the Schwann cells on the nanofibers was examined by SEM (HITACHI SU8010, Japan) to observe the cell adhesion. The samples were cleaned with PBS and treated with UV sterilization. Schwann cells were spread on the nanofiber membrane, fixed with 4% paraformaldehyde for 1 h. The paraformaldehyde was then removed, and the cells were washed twice with PBS. Gradient dehydration was performed with ethanol solutions of different concentrations (30%, 50%, 70%, 80%, 90%, and 100%), with each concentration gradient used for 10 min. The samples were dried at room temperature, sprayed with gold, and viewed using SEM.

Schwann cells were observed and compared on the first, second, and third days by the cell scratch (repair) method. Schwann cells were laid flat on the nanofiber membrane and cross-scratched on the surface with a spearhead. The cells were washed with PBS three times to remove the scratched cells and then added to the medium and cultured in an incubator. Photographs of the samples were obtained at 24 h, 48 h, and 72 h.

2.4. Evaluation of the Safety and Effectiveness of the Nerve Conduits In Vivo in Rats

2.4.1. Experimental Animals and Grouping. Thirty 8-week-old female Sprague-Dawley rats, weighing 200-220 g, were provided by Weitonglihua Experimental Technology Co., Ltd. The rats were randomly divided into three groups of 10 rats each: the PLGA, PLGA/FK506, and autologous nerve transplantation groups.

2.4.2. Surgical Methods and Procedures. Inhalation anesthesia with 3% isoflurane (RWD Life Science, Shenzhen, China) was administered. After anesthesia, the rats were fixed on the operating table in a prone position. After skin disinfection of the right hind limb, the skin and subcutaneous tissues were cut

layer by layer, and the muscle space was bluntly separated to fully expose the sciatic nerve. The sciatic nerve was cut to 15 mm under a surgical microscope. In the PLGA and PLGA/FK506 groups, the two ends of the sciatic nerve were inserted for 1 mm into each end of the nerve conduit and fixed with an 8/0 medical suture. In the autologous nerve transplantation group, the 15-mm sciatic nerve was rotated 180° and then resutured to the two nerve ends with an 8/0 medical suture. The surgical site was douched with normal saline, the muscle and skin were sutured layer by layer with 4/0 medical sutures, and the skin incision was disinfected with iodophor. The rats were closely monitored for infection after the operation.

2.4.3. Gait Analysis. The gait of each group was recorded and analyzed using a CatWalk XT animal gait analyzer (Noldus, Wageningen, The Netherlands) after 12 weeks. The rats were trained for adaptability in advance, and the formal experiment began after the rats could walk continuously on the track. After the experiment, the normal side footprint length (NPL), the operative side footprint length (EPL), the normal side toe width (NTS), the operative side toe width (ETS), the normal side middle toe distance (NIT), and the operative side middle toe distance (EIT) were measured. The sciatic nerve function index (SFI) was calculated according to the following formula: $\mathrm{SFI} = 109.5\,(\mathrm{ETS} - \mathrm{NTS})/\mathrm{NTS} - 38.3\,(\mathrm{EPL} - \mathrm{NPL})/\mathrm{NPL} + 13.3(\mathrm{EIT} - \mathrm{NIT})/\mathrm{NIT} - 8.8$.

2.4.4. Electrophysiological Examination. After the gait analysis, the rats were anesthetized with a 3% isoflurane inhalation. The rats were fixed in a supine position on the operating table, and the right sciatic nerve and gastrocnemius muscle were exposed. Connective tissue surrounding the sciatic nerve was thoroughly removed under the surgical microscope. The recorded electrodes were inserted into the gastrocnemius muscle, and stimulation electrodes were successively placed at the proximal and distal sciatic nerve anastomosis. The amplitude and latency of the compound muscle action potential (CMAP) were recorded using a Synergy Electrophysiology Instrument (Oxford, UK).

2.4.5. Materials and Fixation. After electrophysiological examination, the regenerated sciatic nerve and gastrocnemius muscle of the rats were completely removed under deep anesthesia, and the rats were euthanized with carbon dioxide. The gastrocnemius muscle was immersed in 4% tissue cell fixative and preserved at 4°C for subsequent Masson staining. The sciatic nerve was immersed in 4% tissue cell fixative and preserved at 4°C for subsequent immunostaining.

2.4.6. Muscle Masson Staining. Muscle specimens were removed from the 4% tissue cell fixative solution. Dehydrated, waxed, and embedded, cross-sections were set to 5-μm section thickness. The sections were collected using antistripping slides. Sections were routinely dewaxed to water and Masson stained. After staining, the samples were dehydrated using anhydrous ethanol, made transparent with xylene, and sealed with neutral gum. Muscle fiber morphology was observed under a Leica DM4B microscope, and the cross-sectional area of the muscle fibers in each group was analyzed using the Image-Pro Plus software.

2.4.7. Neuroimmunology Fluorescence Staining. The nerve specimens were removed from the 4% tissue cell fixative solution (Solarbio), dehydrated, embedded in optimal cutting temperature compound (OCT), and sectionalized in cross-section. The frozen section thickness was set to 12 μm, and the sections were collected on slides. After PBS poaching, it was permeated with 0.5% Triton-X100 and blockaded in 5% bovine serum albumin (BSA). The primary antibodies used were rabbit anti-S100 (1 : 200; Sigma-Aldrich) and mouse anti-NF200 (1 : 200; Sigma-Aldrich). After incubation at 4°C overnight, secondary antibodies were Alexa Fluor 594 antirabbit IgG (1 : 200, ZSGB-BIO) and Alexa Fluor 488 antimouse IgG (1 : 200, ZSGB-Bio). The nuclei were stained with 4',6-diamidino-2-phenylindole (DAPI).

2.5. Statistical Analysis. SPSS 26.0 software (IBM Corp., NY, USA) was used for statistical analysis, and $\bar{x}\pm s$ was used to represent quantitative data. The one-way analysis of variance (ANOVA) was used for comparisons between groups. $P < 0.05$ indicated statistical difference, and $P < 0.01$ indicated significant statistical difference.

2.6. Ethics Approval. This study was approved by the Ethics Review Board of the Peking University People's Hospital (2019PHE038) on November 11, 2019, and followed the relevant guidelines.

3. Results

3.1. Physical and Chemical Properties of Enriched FK506 Electrospinning PLGA Nanofiber Membranes and Nerve Conduits. In this study, PLGA and PLGA/FK506 nanofiber membranes were prepared by electrostatic spinning technology, and neural conduits were prepared accordingly (process shown in Figures 1(a)–1(c)). SEM shows that the two nanofiber membranes were uniform and flat, with good nanofiber morphology, as shown in Figures 1(c) and 1(f). The average diameter of the PLGA nanofibers was 0.67 ± 0.16 μm (Figure 1(d)), and that of the PLGA/FK506 nanofibers was 0.68 ± 0.18 μm (Figure 1(g)). This slight increase may have been due to the addition of FK506.

Figure 1(h) shows the stress-strain curves of the PLGA and PLGA/FK506 nanofibers. A mechanical test can reflect the motor mechanical properties of the nanofibers and imitate the changes in the nerve conduits with the movement of the rat when walking. The tensile test results show that the mechanical strength of the nanofibers decreased slightly after the addition of FK506.

FTIR characterization further confirmed the chemical structure of the nanofibers (Figure 1(i)). As shown in Figure 1(d), the characteristic absorption peaks of the PLGA nanofibers are between 1758 cm^{-1} and 1455 cm^{-1} due to the C=O and -CH_2 stretching vibrations. The characteristic absorption peak at 1387 cm^{-1} was due to the stretching vibration of -CH_3. The characteristic absorption peaks at 1183 cm^{-1} and 1083 cm^{-1} were due to the asymmetric stretching vibration of C-O-C in the ester group. PLGA/FK506 had the same characteristic absorption peak as PLGA, indicating that the addition of FK506 did not affect the chemical structure of PLGA.

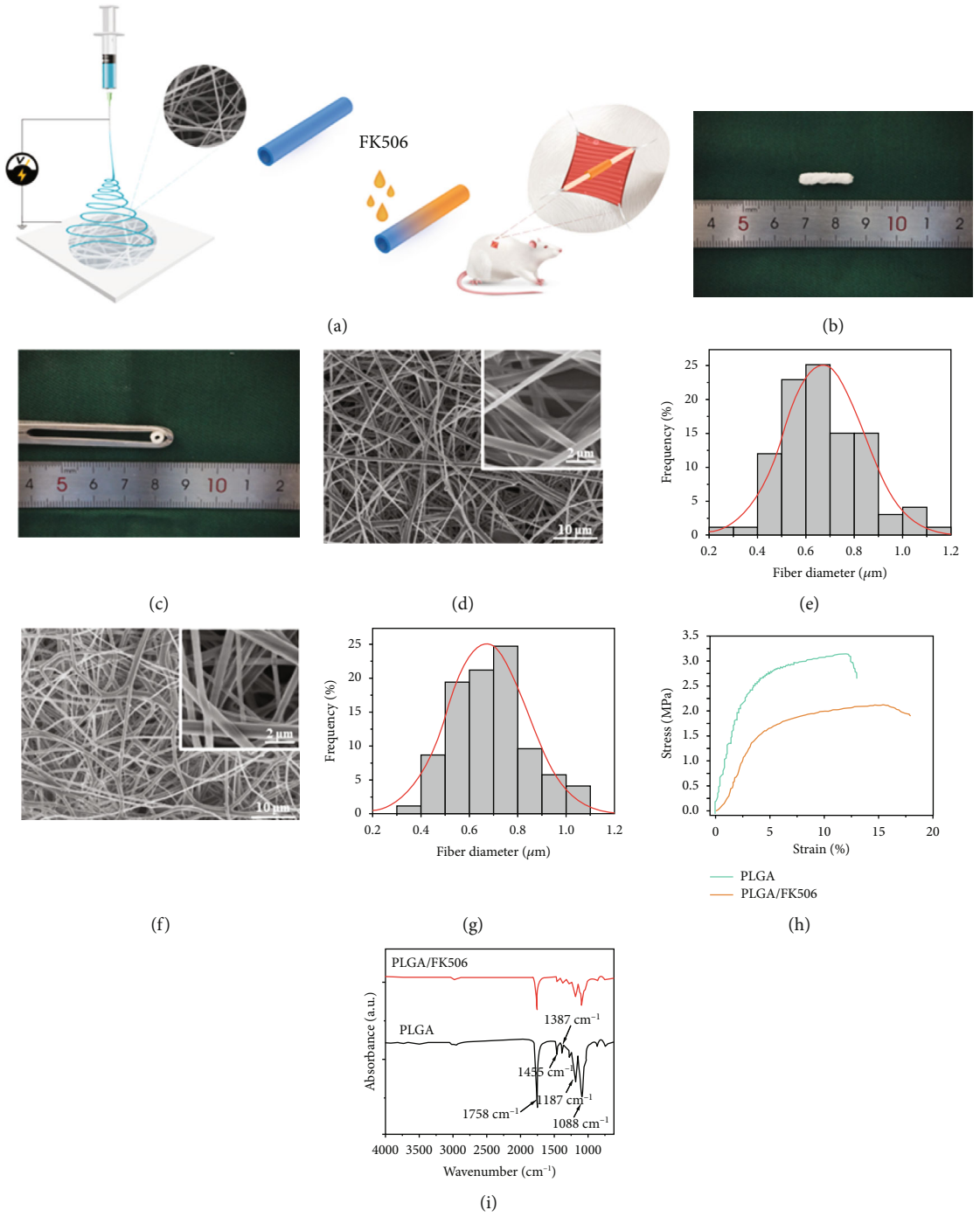

Figure 1: Preparation of nanofiber membranes and nerve conduits. (a) Experimental process. (b and c) Macroscopic views of the conduits. (d and e) SEM morphology and fiber diameter distribution of the PLGA nanofiber membrane ($n = 100$). (f and g) SEM morphology and fiber diameter distribution of the PLGA/FK506 nanofiber membrane ($n = 100$). (h and i) Tensile properties of the nanofibers and the FTIR spectra.

These results indicate that the addition of FK506 had no significant effect on the physical and chemical properties of the PLGA nanofibers and that PLGA retains its good mechanical properties and other advantages.

3.2. Performance Evaluation of In Vitro Degradation and Drug Release of the Nerve Conduits. The weight loss rate and change in material morphology during the degradation process are important characteristics of the material degradation properties. It can be seen from Figure 2(a) that the nanofibers gradually became thicker and that adhesiveness occurred during the degradation process. According to the weight loss rate of the material in Figure 2(b), the degradation of the nanofiber membrane did not change significantly in the first two weeks, but began to gradually degrade from the third week. By the fifth week, the degradation degree

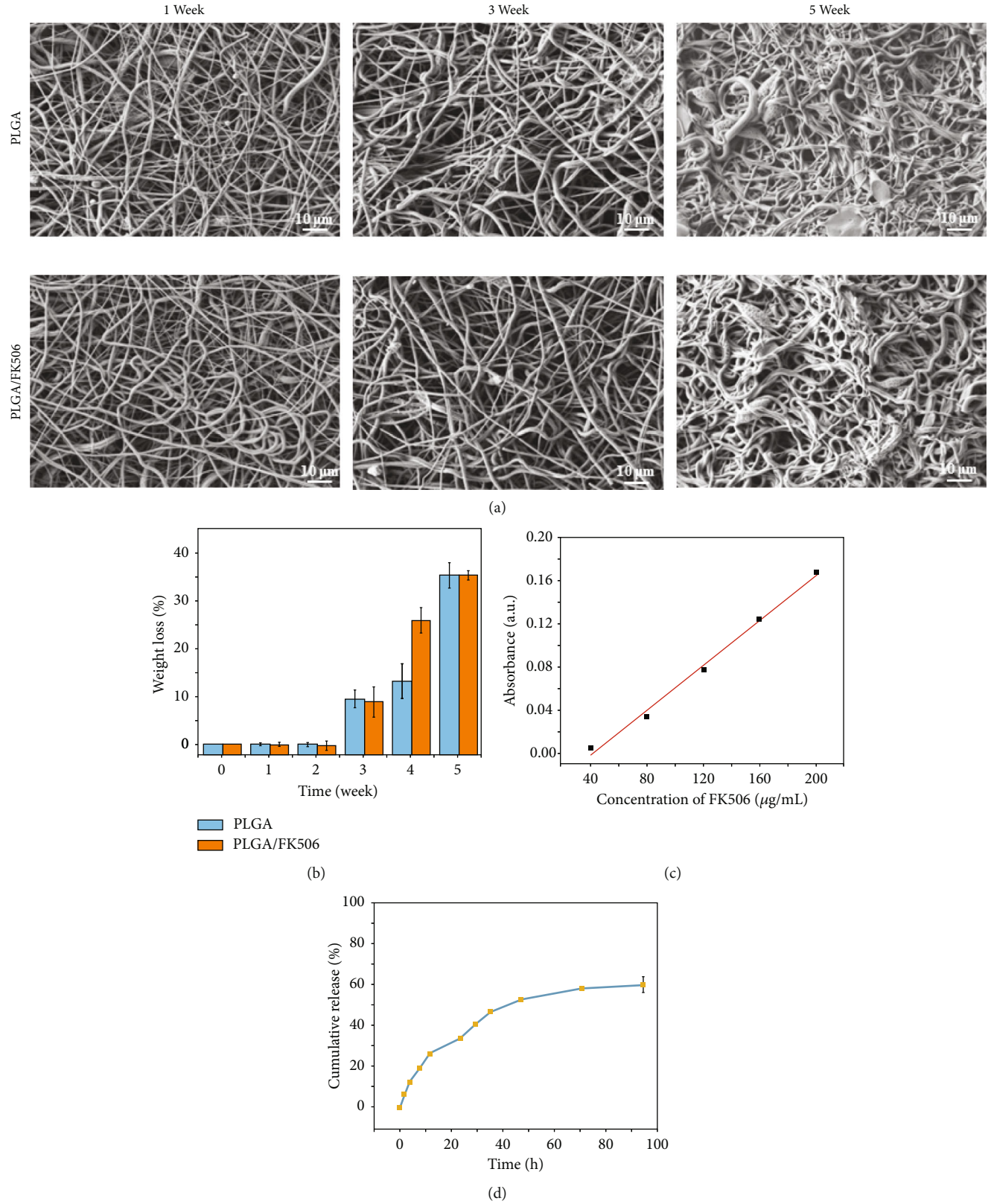

Figure 2: Degradation and release of nanofibers in vitro. (a) SEM diagram of the degradation process of PLGA and PLGA/FK506 nanofibers at the 1 week, 3 weeks, and 5 weeks. (b) Degradation rate of the two nanofibers after 5 weeks. (c) Standard release curves of FK506. (d) Drug release process of the PLGA/FK506 nanofiber membrane.

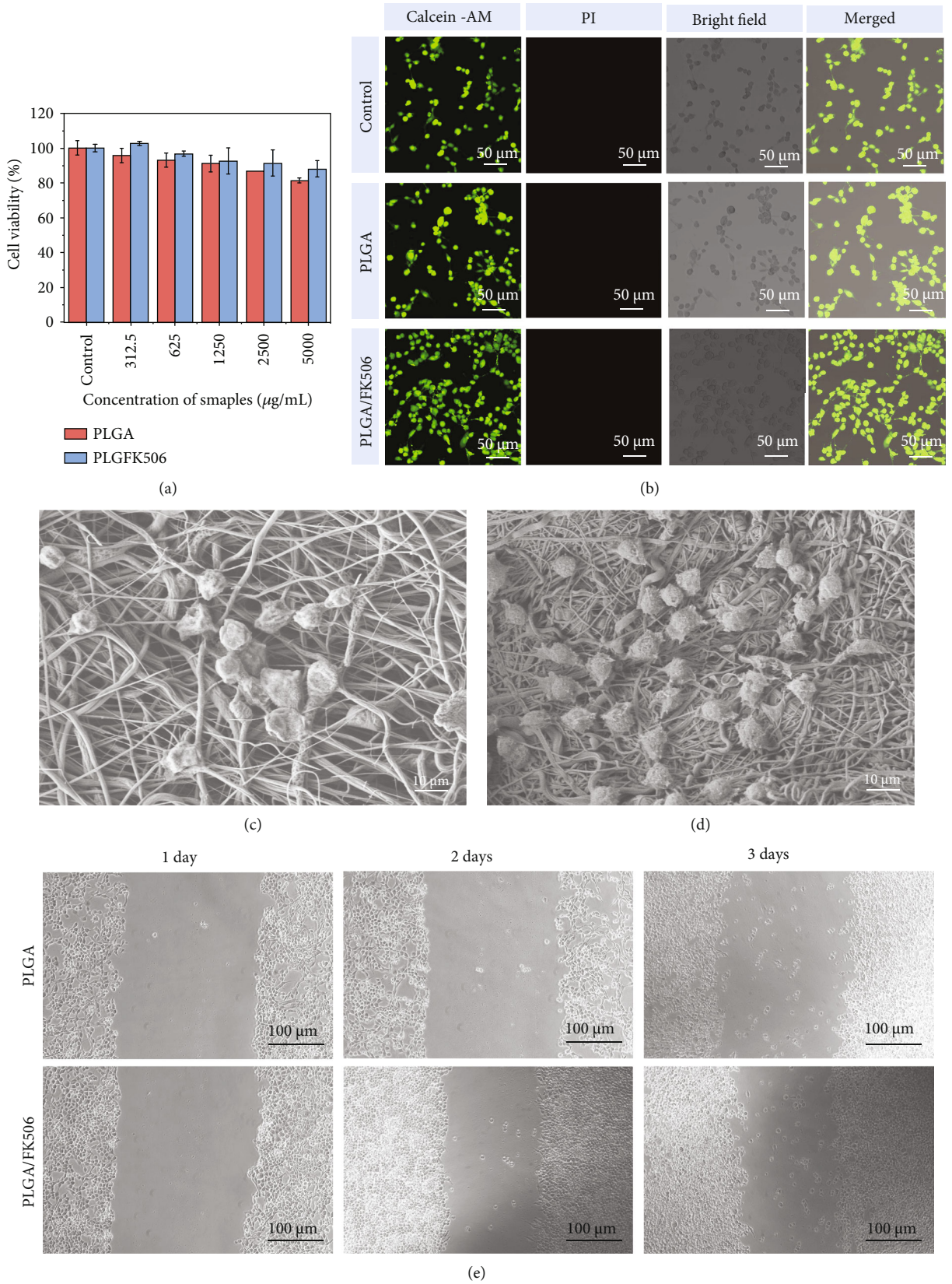

Figure 3: Tests of safety and efficacy of different nanofibers in vitro. (a) Cell activity analysis. (b) Cell viability staining analysis. (c) Cell adhesiveness on PLGA nanofiber membrane. (d) Cell adhesiveness on PLGA/FK506 nanofiber membrane. (e) Cell migration image on different fiber surfaces.

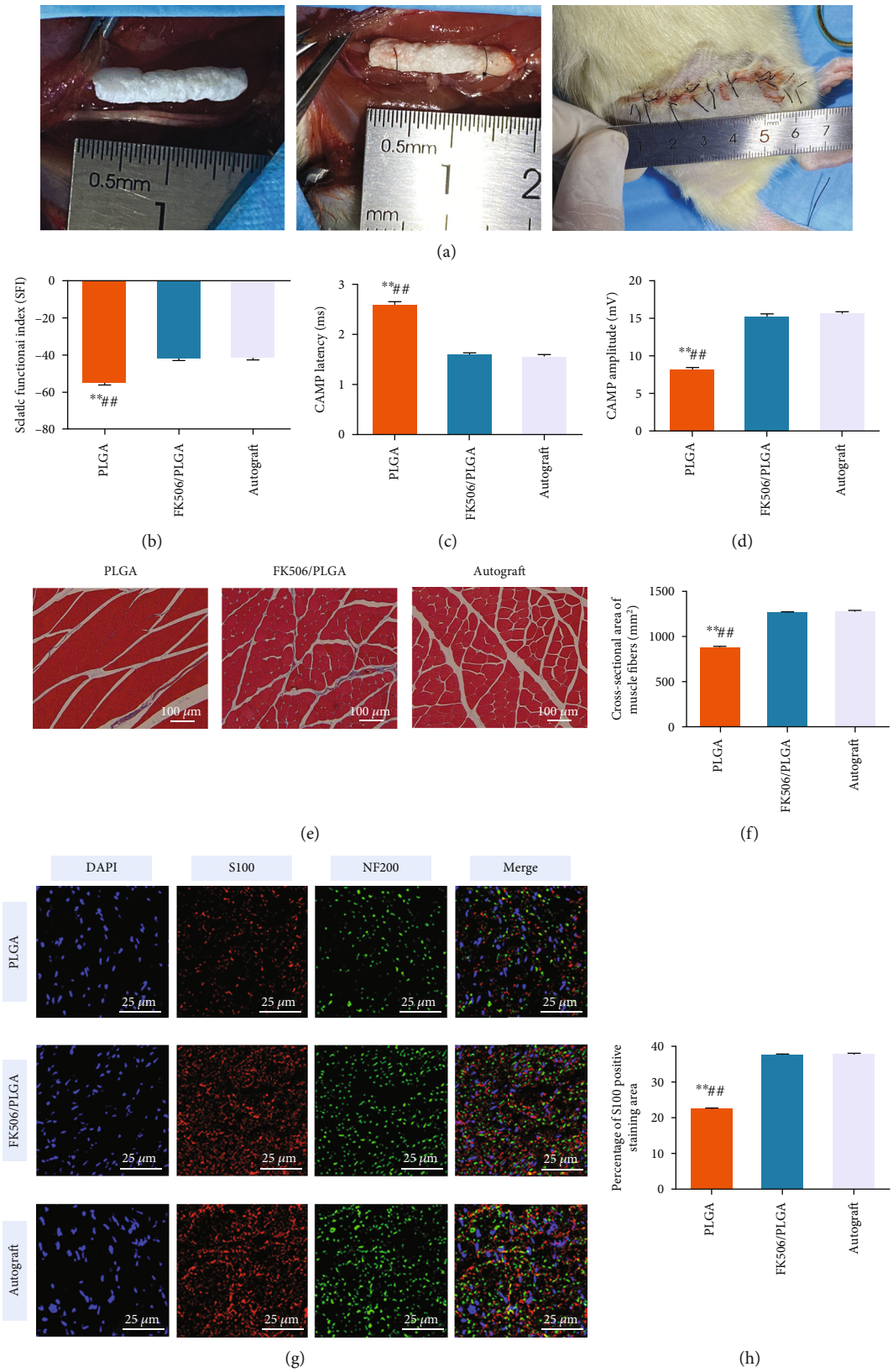

Figure 4: Continued.

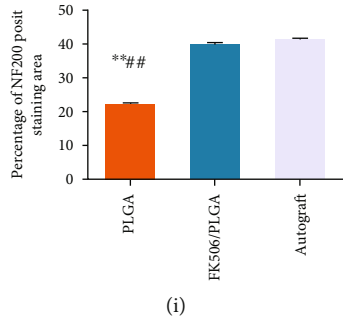

(i)

Figure 4: Comparison of experimental results in vivo in rats. (a) Surgical experiment process on rats. (b) Function index of the sciatic nerve after 12 weeks in each group. (c) Amplitude of the compound muscle action potential after 12 weeks in each group. (d) Incubation period of the compound muscle action potential after 12 weeks in each group. (e) Masson staining diagram of the target muscle (gastrocnemius) after 12 weeks in each group. (f) Statistical diagram of the cross-sectional area of the muscle fiber in each group. (g) Immunofluorescence staining diagram of the nerve. (h) S100 positive area graph. (i) NF200 positive area graph. Note: $n = 10$, **compared with the PLGA/FK506 group, $P < 0.01$; ## compared with the autologous transplantation group, $P < 0.01$.

was 35.2%. These results indicate that the two nanofibers have good degradability and can be used as stable passages for support during nerve repair.

The release control of FK506 is related to the time node and cycle of its action, which ultimately affects the results of nerve repair. The release process of FK506 from the PLGA nanofibers is shown in Figure 2(d). Burst release of FK506 occurred at the beginning of the process. After 12 h the release reached 26.31%, and after 48 h, the release reached 52.98%, and it then gradually stabilized.

3.3. Evaluation of the Safety and Effectiveness of Nerve Conduits in Cell Experiment. The biocompatibility of the materials used for nerve conduits has always been a focus and is an important evaluation index of biomaterials. In this study, MTT analysis and cell viability staining were used to evaluate the biocompatibility of the PLGA/FK506 nanofibers. As shown in Figure 3(a), the survival rate is higher than 80% after the nanofibers and cells of PLGA and PLGA/FK506 were co-cultured. As shown in Figure 3(b), nanofiber-treated cells show green fluorescence according to the cell viability staining analysis, indicating good biocompatibility. Concurrently, to some extent, the above results show that FK506 is beneficial for the proliferation of Schwann cells.

To verify that a PLGA neural scaffold with FK506 could better promote the adhesion of Schwann cells, we conducted the following experiments. Schwann cells grew and spread well on the surface of the PLGA/FK506 nanofibers, and the number of cells on the surface of the PLGA/FK506 nanofibers was higher than that on the surface of the PLGA nanofibers (Figures 3(a) and 3(d)). Meanwhile, the cell migration results (Figure 3(e)) showed that there were far more Schwann cells on the scratch surface of the PLGA/FK506 nanofibers, indicating that FK506 had a better guiding and promoting effect on Schwann cell growth and migration.

These results suggest that the addition of FK506 to PLGA nanofibers reduced cytotoxicity; improved biocompatibility; and promoted the adhesiveness, proliferation, and migration of Schwann cells. PLGA nanofiber with added FK506 is more suitable as a biological material for the constructing neural conduits.

3.4. Evaluation of Safety and Effectiveness of the Nerve Conduits In Vivo in Rats. The evaluation of the PLGA/FK506 nerve conduits, combined with a small sleeve suture technique for sciatic nerve injury repair in rats, has progressed further in Figure 4(a). The performance and repair effects of the prepared nerve conduits were observed for 12 weeks.

The SFI results were obtained by recording and analyzing the gaits of the rats. SFI results closer to zero indicate better functional recovery. As shown in Figure 4(b), the SFI in the PLGA group is lower than that in the PLGA/FK506 and the autologous transplantation groups, and the difference is statistically significant ($P < 0.01$). There was no statistically significant difference in SFI between the PLGA/FK506 and the autologous transplantation group ($P > 0.05$). Currently, CMAP is currently widely used by domestic and foreign scholars as an indicator of the effectiveness of peripheral nerve repair. Its peak amplitude is associated with the number of muscle fibers innervated, while its delay time is associated with the regeneration of the nerve myelin sheath thickness. The CMAP reflects the regeneration of motor nerves in the injured nerve and recovery of target muscle function comprehensively. Figure 4(c) shows that the CMAP delay time in the PLGA group was greater than that in the PLGA/FK506 and the autologous transplantation groups; the difference was statistically significant ($P < 0.01$), whereas there was no significant difference in the CMAP delay time between the PLGA/FK506 and the autologous transplantation groups ($P > 0.05$). Figure 4(d) shows that the amplitude of CMAP in the PLGA group was significantly smaller than that in the PLGA/FK506 and autologous transplantation groups ($P < 0.01$). There was no statistical difference in the CMAP amplitude between the PLGA/FK506 and the autologous transplantation groups ($P > 0.05$). These results indicate that neurological function recovery in the PLGA/FK506 group was close to that of the autologous transplantation group and far better than that in the PLGA group.

As gastrocnemius muscle innervation is dominated by the sciatic nerve, recovery of the gastrocnemius muscle may also indicate recovery of nerve function. As shown in

Figures 4(e) and 4(f), the cross-sectional area of the muscle fiber of the PLGA group is significantly smaller than that of the PLGA/FK506 and the autologous transplantation groups ($P < 0.01$). There was no significant difference between the PLGA/FK506 and autologous transplantation groups ($P > 0.05$). The cross-sectional area of the target muscle fiber can also reflect the state of nerve reinnervation of the target muscle. These results indicated that neurological function recovery in the PLGA/FK506 group was similar to that in the autologous transplantation group and far better than that in the PLGA group.

As showed by immunofluorescence staining in Figure 4(g), Schwann cells are marked by red S100 and neurons by green NF200. As shown in Figures 4(h) and 4(i), the positive area ratios of S100 and NF200 in the PLGA group are both significantly smaller than those in the PLGA/FK506 and autologous transplantation groups ($P < 0.01$). In contrast, there were no significant differences in the S100 and NF200 positive area ratios between the PLGA/FK506 and autologous transplantation groups ($P > 0.05$). These results indicated that the quality of the regenerated nerve in the PLGA/FK506 group was similar to that in the autologous transplantation group and much better than that in the PLGA group.

4. Discussion

Autologous nerve transplantation is the gold standard treatment for repair and regeneration after peripheral nerve injury [24]. The disadvantages of this technique include the limited availability of autologous peripheral nerve tissue for transplantation and donor site morbidity, such as localized anesthetic regions and painful neuroma formation [25]. Therefore, there is a need for new treatments that can replace autologous nerve grafting. Neural conduits have become the best alternative to autologous nerve transplantation for the repair of PNI [26]. Injured nerve regeneration is limited to long-distance nerve defects [27].

After peripheral micro nerve injury, the changes in the local microenvironment of the injured nerve have a significant influence on the repair process and results. Increasing attention has been paid to the establishment of the local microenvironment to improve the repair effect by the exogenous addition of drugs, cellular matrix molecules, or neurotrophic factors, through conduits. The influence of an excessive immune response in the early stage of PNI on the final recovery effect has been brought into prominent focus already [28]. FK506 is a commonly used immunosuppressive drug, and its ability to promote peripheral nerve regeneration is well-established. This is mainly manifested in the following four aspects [29, 30]. First, when FK506 acts on PNI, it can significantly inhibit the expression of IL-6 and the activation of NF-κB in the spinal cord neurons of the injured nerve, which plays an important role in reducing the apoptosis of the injured neurons [31]. Second, FK506 can inhibit fibroblast growth and indirectly promote the proliferation of Schwann cells [29]. Concurrently, FK506 significantly inhibits the local inflammatory response in PNI and reduces the damage caused by the inflammatory response to regenerated axons [29]. Finally, FK506 increases the phosphorylation of GAP-43 through the biological activity of FKBP52 and enhances the activity of growth cones, thereby exerting neurotrophic and neuroprotective effects and promoting the regeneration of neural axons [32]. The effectiveness of FK506 in promoting the regeneration of PNI was also verified in our study. In our study, the PLGA/FK506 group achieves better nerve regeneration results than the PLGA group, as shown in Figure 4, and also confirms the role of FK506 in peripheral nerve repair. In addition, a variety of neurotrophic factors, such as nerve growth factor (NGF), brain-derived neurotrophic factor (BDNF), ciliary neurotrophic factor (CNTF), and vascular endothelial growth factor (VEGF), are beneficial for nerve repair, but their use is limited by the instability and short half-life of nerve factors [33, 34]. To this end, short peptides with cellular properties have been used to simulate the function of nutritional factors, and peptides are stable at different pH values, temperatures, and other environments. Rao et al. added a modified RGI peptide (Ac-RGIDKRHWNSQGG) and KLT peptide (Ac-KLTWQELYQLKYKGIGG) into the interior of the nerve conduit. BDNF and VEGF were simulated, and good results were achieved in repairing sciatic nerve defects in rats [35]. The repair process of PNI involves precise cooperation and complex interactions between numerous cells and molecules. The optimal drug treatment for nerve injury has not yet been determined yet. Therefore, methods for screening the appropriate combination and ratio of many drugs are also worthy of further research and attention.

In addition to the various factors and drugs that promote nerve repair, a sustained release carrier loaded with the drugs is also crucial for the effectiveness of the drugs. The selection of carrier materials and drug loading methods should be considered when constructing of carriers. Aliphatic polyesters are typical degradable polymers that can be used for nerve repair, also for poly (L-lactic acid) (PLLA), poly (glycolic acid) (PGA), polycaprolactone (PCL), and poly (L-lactic co-glycolic acid) (PLGA). Owing to their good mechanical properties and plasticity in physical and chemical properties, these materials are often used as carriers for constructing neural conduits, either alone or in combination with other materials. Among them, PLGA has been widely used in clinical practice for wound sutures, as certified by the FDA [14–16]. PLGA is a well-known polymer, with properties such as good biocompatibility, well-defined biodegradability, and ease of fabrication and has a wide range of applications in biomedical engineering [35]. The advantage of the PLGA nerve conduit is that it is degradable and does not require a second surgery for removal after nerve regeneration. Studies have shown that PLGA has an optimal degradation time which provides sufficient mechanical support for nerve regeneration without hindering nerve regeneration. Previous studies have also shown that PLGA is a suitable material for a nerve conduits [36]. In this study, the degradation of PLGA electrospun nanofibers in vitro is shown in Figure 2(a), indicating its effective support for peripheral nerve regeneration and its excellent degradability.

The drug loading methods of nerve conduits have also been well-studied, from the direct soaking method to the use of nanofibers from electrostatic spinning uniformly distributing factors or drugs in carriers. Later, other methods were developed, such as modification of the surface groups of the carrier, polypeptide crosslinking, multicoating embedding, and canal packing using different materials. However, this increases the complexity of the conduit preparation process and the production transformation. By constructing a RADA16-I-BMHP1 assembled peptide and PLGA composite nanomaterial scaffold, Nune et al. improved the mechanical properties and degradation rate of solitary RADA16-I-BMHP1 assembled peptide scaffolds and promoted the adhesiveness, proliferation, migration, and neural-related gene expression of Schwann cells [37]. Oh et al. prevented invasion of the nerve tissue and concurrently supported the growth of blood vessels by constructing PLGA neural conduits with different pore sizes in the internal and external walls, facilitating the exchange of nutrients and metabolites [38]. In addition to PLGA, Yun Qian applied 3D printing and layer-by-layer casting to construct a graphene-PCL compound nerve conduit with its surface modified by polydopamine (PDA) and arginylglycylaspartic acid (RGD), and such studies related to sciatic nerve repair in rats have been conducted. It significantly promotes the expression and repair of PNI from multiple perspectives, such as electrical conductivity and drug effect [39].

Electrospun nanofibers have great potential for use as regenerative medical scaffolds owing to their permeability, which is structurally similar to the extracellular matrix [40]. Electrospun nanofibers can be used to guide cell morphology, migration, and differentiation. In this study, electrostatic spinning technology was applied to construct a FK506-enriched PLGA nanofiber neural conduit, which further improved its biocompatibility on the premise that physicochemical properties such as PLGA morphology and surface groups were not affected, and mechanical properties were retained. The release process of FK506 in PLGA electrospun nanofibers is shown in Figure 2, which demonstrates that the burst release of FK506 occurred at the beginning of the process and that the release amount reached 52.98% after 48 h and then gradually stabilized. Concurrently, the in vivo and in vitro experiments verify that the PLGA/FK506 nanofibers had better repair effectiveness in nerve injury and further improved the quality of nerve regeneration and repair, as shown in Figure 3. Good performance, the loaded drug, and drug release of the nerve conduit have a great influence on the quality of regeneration and repair in nerve injury.

This study had some limitations. First, although electrospun PLGA as an artificial material simulates the extracellular membrane, it still requires improvement in many respects; for example, other biomaterials can be combined with the electrospun PLGA neural conduit. Second, although the effectiveness of FK506 in nerve regeneration has been universally recognized by many researchers, its mechanism of action when aligned with electrospun PLGA in promoting nerve repair (such as an anti-inflammatory mechanism) in this experiment needs to be further studied from the perspective of immunology and molecular biology in the future. In addition, the FK506-enriched electrospun PLGA used in this study can be further validated by animal experiments in larger mammals or primates.

5. Conclusion

This study sought to apply electrostatic spinning technology to the preparation of an FK506-enriched nanomaterial conduit and to prove its safety and effectiveness. This new conduit was successfully used to repair long-distance sciatic nerve injury in rats. This study demonstrates an effective way to repair long-distance peripheral nerve injuries with potential clinical applications in the future.

Abbreviations

PNI: Peripheral nerve injury
FK506: Tacrolimus
PLGA: Poly (lactic-co-glycolic acid)
DMSO: Dimethyl sulfoxide
SEM: Scanning electron microscopy
PBS: Phosphate buffered saline
MTT: 3-(4,5-Dimethylthiazol-2-yl)-2,5-diphenyltetrazolium bromide
DMEM: Dulbecco's modified eagle medium
OD: Optical density
NPL: Normal side footprint length
EPL: Operative side footprint length
NTS: Normal side toe width
ETS: Operative side toe width
NIT: Normal side middle toe distance
EIT: Operative side middle toe distance
SFI: Sciatic nerve function index
CMAP: Compound muscle action potential
OCT: Optimal cutting temperature compound
BSA: Bovine serum albumin
DAPI: 4',6-Diamidino-2-phenylindole
NGF: Nerve growth factor
BDNF: Brain-derived neurotrophic factor
CNTF: Ciliary neurotrophic factor
VEGF: Vascular endothelial growth factor
PLLA: Poly (L-lactic acid)
PGA: Poly (glycolic acid)
PCL: Polycaprolactone
PDA: Polydopamine
RGD: Arginylglycylaspartic acid.

Data Availability

The data generated and/or analyzed during the current study are not publicly available for legal/ethical reasons but are available from the corresponding author on reasonable request.

Conflicts of Interest

The authors declare that they have no conflicts of interest.

Authors' Contributions

All authors contributed to the conception, writing, critical review, and revision of the manuscript. Tingmin Xu, Ming Li, and Jianjun Li have contributed to the conceptualization; Ming Li, Hongyu Chu, and Guo Wei have contributed to the methodology; Zuliyaer Talifu and Han Ke have contributed to the software; Tingmin Xu, Yunzhu Pan, and Xu Xin have contributed to the validation; Tingmin Xu and Yanhua Wang have contributed to the formal analysis; Ming Li, Feng Gao, and Jianjun Li have contributed to the investigation; Feng Gao and Jianjun Li have contributed to the resources; Hongyu Chu, Chuanlin Wang, and Feng Gao have contributed to the data curation; Tingmin Xu and Hongyu Chu have contributed to the writing—original draft preparation; Tingmin Xu, Ming Li, and Feng Gao have contributed to the writing—review and editing; Ming Li and Zuliyaer Talifu have contributed to the visualization; Jianjun Li has contributed to the supervision; Tingmin Xu and Feng Gao have contributed to the project administration; Feng Gao and Jianjun Li have contributed to the funding acquisition. Ting-Min Xu, Hong-Yu Chu, and Ming Li contributed equally to this work.

Acknowledgments

The authors thank the members in Beijing Key Laboratory of Neural Injury and Rehabilitation and National Center for Trauma Medicine, China. This work was supported by the National Natural Science Foundation of China [Grant No.31640045], the National Natural Science Foundation of China [Grant No. 81901251], the National Natural Science Foundation of China [Grant No. 82071400], the Beijing Natural Science Foundation [Grant No. 7204323], and the Science Foundation of China Rehabilitation Research Center [Grant No. 2019ZX-Q1].

References

[1] P. X. Zhang, N. Han, Y. H. Kou et al., "Tissue engineering for the repair of peripheral nerve injury," *Neural Regeneration Research*, vol. 14, no. 1, pp. 51–58, 2019.

[2] M. L. Wang, M. Rivlin, J. G. Graham, and P. K. Beredjiklian, "Peripheral nerve injury, scarring, and recovery," *Connective Tissue Research*, vol. 60, no. 1, pp. 3–9, 2019.

[3] M. Modrak, M. A. H. Talukder, K. Gurgenashvili, M. Noble, and J. C. Elfar, "Peripheral nerve injury and myelination: potential therapeutic strategies," *Journal of Neuroscience Research*, vol. 98, no. 5, pp. 780–795, 2020.

[4] G. Hussain, J. Wang, A. Rasul et al., "Current status of therapeutic approaches against peripheral nerve injuries: a detailed story from injury to recovery," *International Journal of Biological Sciences*, vol. 16, no. 1, pp. 116–134, 2020.

[5] S. Vijayavenkataraman, "Nerve guide conduits for peripheral nerve injury repair: a review on design, materials and fabrication methods," *Acta Biomaterialia*, vol. 106, no. 1, pp. 54–69, 2020.

[6] Q. Long, B. Wu, Y. Yang et al., "Nerve guidance conduit promoted peripheral nerve regeneration in rats," *Artificial Organs*, vol. 45, no. 6, pp. 616–624, 2021.

[7] B. Wang, C. F. Lu, Z. Y. Liu et al., "Chitin scaffold combined with autologous small nerve repairs sciatic nerve defects," *Neural Regeneration Research*, vol. 17, no. 5, pp. 1106–1114, 2022.

[8] F. Rao, Z. Yuan, D. Zhang et al., "Small-molecule SB216763-loaded microspheres repair peripheral nerve injury in small gap tubulization," *Frontiers in Neuroscience*, vol. 13, no. 13, p. 489, 2019.

[9] P. Meena, A. Kakkar, M. Kumar et al., "Advances and clinical challenges for translating nerve conduit technology from bench to bed side for peripheral nerve repair," *Cell and Tissue Research*, vol. 383, no. 2, pp. 617–644, 2021.

[10] Y. Yan, R. Yao, J. Zhao et al., "Implantable nerve guidance conduits: material combinations, multi-functional strategies and advanced engineering innovations," *Bioactive Materials*, vol. 11, no. 5, pp. 57–76, 2022.

[11] N. U. Kang, S. J. Lee, and S. J. Gwak, "Fabrication techniques of nerve guidance conduits for nerve regeneration," *Yonsei Medical Journal*, vol. 63, no. 2, pp. 114–123, 2022.

[12] Z. Peixun, H. Na, Y. Kou, Y. Xiaofeng, and B. Jiang, "Peripheral nerve intersectional repair by bi-directional induction and systematic remodelling: biodegradable conduit tubulization from basic research to clinical application," *Artificial cells, nanomedicine, and biotechnology*, vol. 45, no. 8, pp. 1464–1466, 2017.

[13] F. Rao, Z. Yuan, M. Li et al., "Expanded 3D nanofibre sponge scaffolds by gas-foaming technique enhance peripheral nerve regeneration," *Artificial cells, nanomedicine, and biotechnology*, vol. 47, no. 1, pp. 491–500, 2019.

[14] P. Lu, G. Wang, T. Qian et al., "The balanced microenvironment regulated by the degradants of appropriate PLGA scaffolds and chitosan conduit promotes peripheral nerve regeneration," *Materials Today Bio*, vol. 12, no. 16, p. 100158, 2021.

[15] M. Okamoto and B. John, "Synthetic biopolymer nanocomposites for tissue engineering scaffolds," *Progress in Polymer Science*, vol. 38, no. 10-11, pp. 1487–1503, 2013.

[16] T. W. Chung, M. C. Yang, C. C. Tseng et al., "Promoting regeneration of peripheral nerves *in-vivo* using new PCL-NGF/Tirofiban nerve conduits," *Biomaterials*, vol. 32, no. 3, pp. 734–743, 2011.

[17] A. C. Pinho, A. C. Fonseca, A. C. Serra, J. D. Santos, and J. F. Coelho, "Peripheral nerve regeneration: current status and new strategies using polymeric materials," *Advanced Healthcare Materials*, vol. 5, no. 21, pp. 2732–2744, 2016.

[18] Z. I. Foraida, T. Kamaldinov, D. A. Nelson, M. Larsen, and J. Castracane, "Elastin-PLGA hybrid electrospun nanofiber scaffolds for salivary epithelial cell self-organization and polarization," *Acta Biomaterialia*, vol. 62, no. 15, pp. 116–127, 2017.

[19] F. Rao, D. Zhang, T. Fang et al., "Exosomes from human gingiva-derived mesenchymal stem cells combined with biodegradable chitin conduits promote rat sciatic nerve regeneration," *Stem cells international*, vol. 2019, no. 2, Article ID e2546367, p. 12, 2019.

[20] S. Liu, L. Zhou, C. Li et al., "Chitin conduits modified with DNA-peptide coating promote the peripheral nerve regeneration," *Biofabrication*, vol. 14, no. 1, 2022.

[21] F. Fregnan, L. Muratori, A. R. Simões, M. G. Giacobini-Robecchi, and S. Raimondo, "Role of inflammatory cytokines in peripheral nerve injury," *Neural Regeneration Research*, vol. 7, no. 29, pp. 2259–2266, 2012.

[22] B. Davis, S. Wojtalewicz, P. Labroo et al., "Controlled release of FK506 from micropatterned PLGA films: potential for application in peripheral nerve repair," *Neural regeneration research*, vol. 13, no. 7, pp. 1247–1252, 2018.

[23] P. Labroo, D. Hilgart, B. Davis et al., "Drug-delivering nerve conduit improves regeneration in a critical-sized gap," *Biotechnology and Bioengineering*, vol. 116, no. 1, pp. 143–154, 2019.

[24] D. Grinsell and C. P. Keating, "Peripheral Nerve Reconstruction after Injury: A Review of Clinical and Experimental Therapies," *BioMed Research International*, vol. 2014, Article ID 698256, 13 pages, 2014.

[25] F. F. A. Ijpma, J. P. A. Nicolai, and M. F. Meek, "Sural nerve donor-site morbidity," *Annals of Plastic Surgery*, vol. 57, no. 4, pp. 391–395, 2006.

[26] S. Houshyar, A. Bhattacharyya, and R. Shanks, "Peripheral nerve conduit: materials and structures," *ACS Chemical Neuroscience*, vol. 10, no. 8, pp. 3349–3365, 2019.

[27] V. Hasirci, D. Arslantunali, T. Dursun, D. Yucel, and N. Hasirci, "Peripheral nerve conduits: technology update," *Medical Devices (Auckland, NZ)*, vol. 7, pp. 405–424, 2014.

[28] A. Baradaran, H. El-Hawary, J. I. Efanov, and L. Xu, "Peripheral nerve healing: so near and yet so far," *Seminars in Plastic Surgery*, vol. 35, no. 3, pp. 204–210, 2021.

[29] K. J. Zuo, T. M. Saffari, K. Chan, A. Y. Shin, and G. H. Borschel, "Systemic and local FK506 (tacrolimus) and its application in peripheral nerve surgery," *The Journal of Hand Surgery*, vol. 45, no. 8, pp. 759–765, 2020.

[30] K. J. Zuo, G. Shafa, K. Chan et al., "Local FK506 drug delivery enhances nerve regeneration through fresh, unprocessed peripheral nerve allografts," *Experimental Neurology*, vol. 341, p. 113680, 2021.

[31] P. Konofaos and J. K. Terzis, "FK506 and nerve regeneration: past, present, and future," *Journal of Reconstructive Microsurgery*, vol. 29, no. 3, pp. 141–148, 2013.

[32] M. Zuber and J. Donnerer, "Effect of FK506 on neurotransmitter content and expression of GAP-43 in neurotoxin-lesioned peripheral sensory and sympathetic neurons," *Pharmacology*, vol. 66, no. 1, pp. 44–50, 2002.

[33] Z. Liu, S. Ma, S. Duan et al., "Modification of titanium substrates with chimeric peptides comprising antimicrobial and titanium-binding motifs connected by linkers to inhibit biofilm formation," *ACS Applied Materials & Interfaces*, vol. 8, no. 8, pp. 5124–5136, 2016.

[34] J. Valencia-Serna, P. Chevallier, R. B. Kc, G. Laroche, and H. Uludağ, "Fibronectin-modified surfaces for evaluating the influence of cell adhesion on sensitivity of leukemic cells to siRNA nanoparticles," *Nanomedicine (London, England)*, vol. 11, no. 9, pp. 1123–1138, 2016.

[35] F. Rao, Y. Wang, D. Zhang et al., "Aligned chitosan nanofiber hydrogel grafted with peptides mimicking bioactive brain-derived neurotrophic factor and vascular endothelial growth factor repair long-distance sciatic nerve defects in rats," *Theranostics*, vol. 10, no. 4, pp. 1590–1603, 2020.

[36] W. Zhao, J. Li, K. Jin, W. Liu, X. Qiu, and C. Li, "Fabrication of functional PLGA-based electrospun scaffolds and their applications in biomedical engineering," *Materials Science & Engineering. C, Materials for Biological Applications*, vol. 59, pp. 1181–1194, 2016.

[37] M. Nune, U. M. Krishnan, and S. Sethuraman, "PLGA nanofibers blended with designer self-assembling peptides for peripheral neural regeneration," *Materials Science & Engineering. C, Materials for Biological Applications*, vol. 62, pp. 329–337, 2016.

[38] S. H. Oh and J. H. Lee, "Fabrication and characterization of hydrophilized porous PLGA nerve guide conduits by a modified immersion precipitation method," *Journal of Biomedical Materials Research. Part A*, vol. 80, no. 3, pp. 530–538, 2007.

[39] Y. Qian, X. Zhao, Q. Han, W. Chen, H. Li, and W. Yuan, "An integrated multi-layer 3D-fabrication of PDA/RGD coated graphene loaded PCL nanoscaffold for peripheral nerve restoration," *Nature Communications*, vol. 9, no. 1, p. 323, 2018.

[40] L. G. Pozzobon, L. E. Sperling, C. E. Teixeira, T. Malysz, and P. Pranke, "Development of a conduit of PLGA-gelatin aligned nanofibers produced by electrospinning for peripheral nerve regeneration," *Chemico-Biological Interactions*, vol. 348, p. 109621, 2021.